

Supporting Information to the paper:

**Stimuli-Responsive Micellar Interpolyelectrolyte Complexes –
Control of Micelle Dynamics *via* Core Crosslinking**

by Eva Betthausen, Markus Drechsler, Melanie Förtsch, Dmitry V. Pergushov, Felix H. Schacher, and Axel H. E. Müller

Interpolyelectrolyte Complex Formation with BMANaDq Precursor Micelles

Complexation with Poly(sodium 4-styrenesulfonate)

In addition to all complexation reactions with commercially available PSSNa with a broad molecular weight distribution, IPEC formation was carried out with a narrowly distributed PSSNa ($M_n = 20\,000$ g/mol, PDI = 1.02). The IPECs were prepared at pH 10 and $Z_{-/+} = 1$ using the non-crosslinked BMANaDq micelles as precursors. The cryo-TEM micrograph of the resulting micellar IPECs in Figure S1 shows a broadening of the micellar size distribution comparable to the complexation with commercial PSSNa.

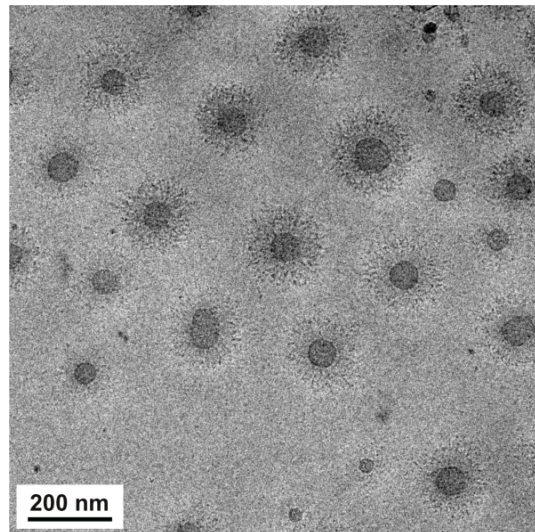


Figure S1: Cryo-TEM micrograph of micellar IPECs from BMANaDq precursor micelles and narrowly distributed PSSNa in aqueous solution at pH 10 and $Z_{-/+} = 1$.

Complexation with Poly(sodium acrylate)

Prior to IPEC formation with PNa-*b*-PNIPAAm diblock copolymers, experiments were carried out using a PNa homopolymer. For this purpose a commercially available PNa

with a molecular weight of $M_w = 1\,250\,000$ g/mol was used. The non-crosslinked BMANaDq precursor micelles were mixed with PNa at pH 10 and $Z_{-/+} = 1$ and the resulting micellar IPECs were analyzed by DLS and cryo-TEM (Figure S2). Both methods show a broadening of the micellar size distribution upon IPEC formation, probably due to rearrangements of the micellar cores as observed during the complexation with PSSNa. Again, the micellar IPECs at $Z_{-/+} = 1$ remain water-soluble. Also here, we assume that overcharging effects are present, as the PNa used is of extremely high molecular weight. Thus, the complexation with PNa might again lead to the formation of “loops” and “trails” and, thus, structures with a negative net charge. The micellar IPECs with PNa exhibit a hydrodynamic radius of $\langle R_h \rangle_z = 99$ nm.

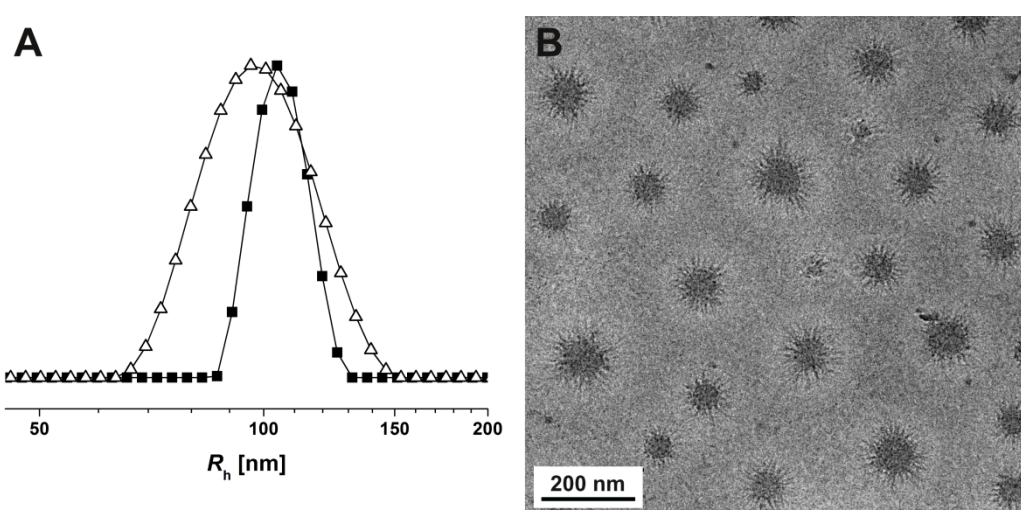


Figure S2: Intensity-weighted DLS CONTIN plots for BMANaDq precursor micelles in aqueous solution at pH 10 (—■—, $\langle R_h \rangle_z = 107$ nm, PDI = 0.06) and micellar IPECs with PNa at $Z_{-/+} = 1$ (—△—, $\langle R_h \rangle_z = 99$ nm, PDI = 0.10) (A); cryo-TEM micrograph of micellar IPECs from BMANaDq and PNa at $Z_{-/+} = 1$ (B).

Complexation with Bis-Hydrophilic PNa-*b*-PNIPAAm Diblock Copolymers

In addition to core-crosslinked micellar IPECs with a PNIPAAm corona obtained through complexation with bis-hydrophilic PNa-*b*-PNIPAAm diblock copolymers, comparable IPECs with non-crosslinked cores were prepared. The IPEC formation was carried out at pH 10 by mixing BMANaDq precursor micelles and ANa₂₇NIPAAm₁₅₀ at $Z_{-/+} = 1$. The DLS CONTIN plot and a cryo-TEM micrograph of the resulting micellar IPECs are shown in Figure S3. The hydrodynamic radius decreases ($\langle R_h \rangle_z = 97$ nm) as compared to the precursor micelles ($\langle R_h \rangle_z = 107$ nm), but nearly coincides with the size found for IPECs with PNa, which can be explained by the collapse of the PDMAEMAq corona upon interpolyelectrolyte complexation. Since the non-crosslinked BMANaDq micelles were used as precursors, again

a broadening of the micellar size distribution upon IPEC formation is observed both in the DLS CONTIN plot and the cryo-TEM micrograph.

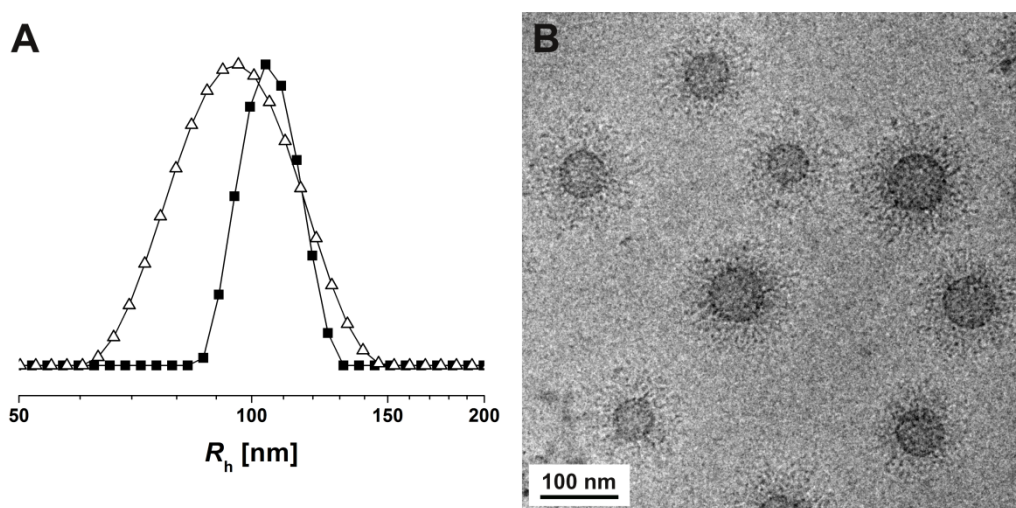


Figure S3: Intensity-weighted DLS CONTIN plots for BMANaDq precursor micelles in aqueous solution at pH 10 (—■—, $\langle R_h \rangle_z = 107$ nm, PDI = 0.06) and micellar IPECs with ANa₂₇NIPAAm₁₅₀ at $Z_{-/+} = 1$ (—△—, $\langle R_h \rangle_z = 97$ nm, PDI = 0.10) (A); cryo-TEM micrograph of micellar IPECs from BMANaDq and ANa₂₇NIPAAm₁₅₀ at $Z_{-/+} = 1$ (B).

The thermo-responsive properties of these structures were investigated *via* turbidity measurements ($c \sim 0.3$ g/L) and temperature-dependent DLS measurements (Figure S4). In both cases, a cloud point of 36 °C could be obtained. A further increase in temperature resulted in the precipitation of the IPEC particles.

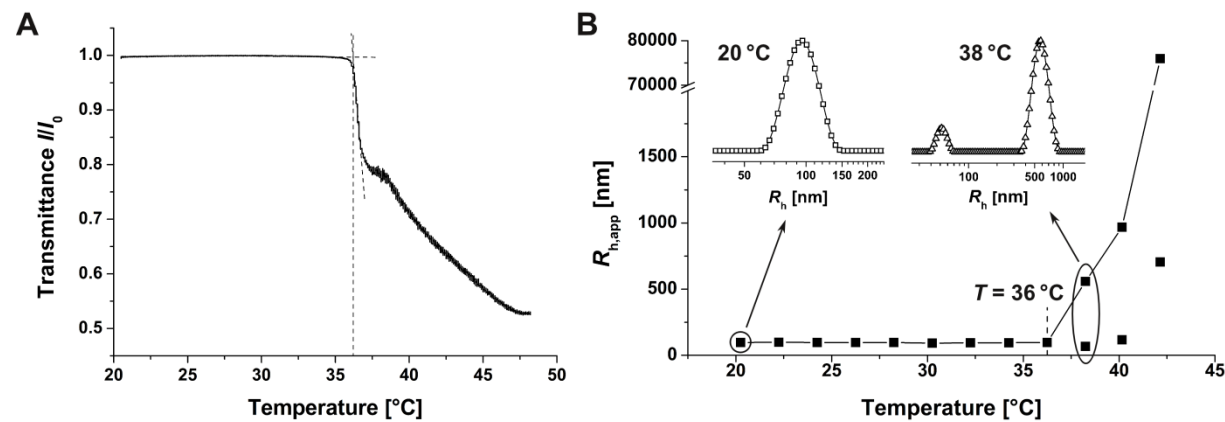


Figure S4: Cloud point determination for micellar IPECs from BMANaDq precursor micelles and ANa₂₇NIPAAm₁₅₀ at $Z_{-/+} = 1$ in aqueous solution at pH 10 *via* turbidity measurements ($c \sim 0.3$ g/L) (A); dependence of hydrodynamic radius of micellar IPECs on the temperature as determined by DLS (B); the insets show intensity-weighted DLS CONTIN plots for the micellar IPECs at different temperatures; 20 °C (—□—, $\langle R_h \rangle_z = 97$ nm, PDI = 0.10) and 38 °C (—△—, $R_{h,app} = 68$ nm and 553 nm); the onset of aggregation is highlighted at 36 °C.